

Quantum Noise in Gravitational-wave Interferometers: Overview and Recent Developments

Thomas Corbitt and Nergis Mavalvala¹

Massachusetts Institute of Technology, 175 Albany Street, Cambridge, MA 02139

ABSTRACT

We present an overview of quantum noise in gravitational wave interferometers. Gravitational wave detectors are extensively modified variants of a Michelson interferometer and the quantum noise couplings are strongly influenced by the interferometer configuration. We describe recent developments in the treatment of quantum noise in the complex interferometer configurations of present-day and future gravitational-wave detectors. In addition, we explore prospects for the use of squeezed light in future interferometers, including consideration of the effects of losses, and the choice of optimal readout schemes.

Keywords: Quantum noise, quantum non-demolition, gravitational waves, interferometers

1. INTRODUCTION

With several gravitational wave (GW) observatories worldwide nearing completion,¹ the direct detection of gravitational waves (GWs) from astrophysical sources is a rapidly growing enterprise. The Laser Interferometer Gravitational-wave Observatory (LIGO) is the US component of this worldwide effort. Even as the first generation detectors are being commissioned,² design and planning is well underway for next-generation detectors, with installation to begin as early as 2007. The initial detectors have their maximal strain sensitivity between 40 Hz and 7 kHz, while the advanced detectors are expected to be a factor of 10 to 15 more sensitive in a band from 10 Hz to 7 kHz.³ Third generation interferometers are still in the earliest stages of theoretical development⁴ and table-top testing.⁵ In this paper we will systematically survey the *quantum mechanical* noise in a broad sampling of these interferometers and discuss the implications for the increasingly important role that quantum optics and quantum information are likely to play in advanced GW interferometers.

Most gravitational-wave (GW) interferometers, such as those used LIGO, are variants of a Michelson interferometer. The Michelson interferometer makes it natural to decompose the optical fields and the corresponding motion of the arm-cavity mirrors into symmetric and antisymmetric modes. Since the Michelson is operated on the dark fringe, ideally only optical signals induced by the antisymmetric motion of the arm-cavity mirrors exit the antisymmetric – or output – port of the beam splitter. The motion of the mirrors that generates an optical signal at the output port may be due to a variety of instrumental noise sources that compete with the mirror displacements a passing GW would induce.

Noise sources that impose limits on the strain sensitivity of the detector include seismic noise due to terrestrial vibrations at low frequencies, thermal noise due to thermally driven fluctuations of the mirrors at intermediate frequencies and shot noise due to fluctuations in photon number at high frequencies. In the initial detectors these are indeed the limiting noise sources. In advanced detectors, however, the sensitivity at almost all frequencies in the detection band is expected to be limited by *quantum* noise, primarily due to the increase in circulating laser power, but also strongly influenced by the detailed optical configuration used.

¹Send correspondence to Nergis Mavalvala. E-mail: nergis@ligo.mit.edu, Telephone: 1 617 253-5657

1.1. Sources of Quantum Noise

Quantum noise refers to a broad class of noise sources that arise from the quantum nature of the light source and photodetection process used in GW interferometers. We shall consider three types of quantum noise in this review:

- *Radiation-pressure noise* arises from uncertainties in the mirror positions due to quantum fluctuations exerting fluctuating radiation pressure on the mirrors. It was shown over two decades ago that this radiation pressure force can be attributed to vacuum fluctuations that enter the unused ports of the interferometer.^{6, 7} We shall continue our analysis in this framework.
- *Shot noise* arises from uncertainty due to quantum mechanical fluctuations in the number of photons at the interferometer output.
- *Test-mass quantization* noise arises from uncertainty due to intrinsic quantization of the position and momenta of the mirrors. However, it has been shown that non-zero contributions to the detector output commutator from test-mass (mirror) quantization exactly cancel the the non-zero contributions from the radiation-pressure and shot noise commutation relations, and thus the test mass quantization does not limit the measurement process at all.⁸

1.2. The Standard Quantum Limit

The standard quantum limit (SQL) is a well-known and well-used quantity in quantum optics as well as in quantum measurement theory. While closely related, the SQL has a different interpretation in these two fields. For gravitational wave detectors – where photons are used to measure the positions of the test-mass mirrors – the SQL is obtained by exactly balancing the radiation-pressure induced position fluctuations with measurement uncertainty due to fluctuations in the number of photons, or shot noise.⁹ This balance is nothing but a statement of the Heisenberg uncertainty principle (HUP) for the position and momentum of the particle: an initial measurement of the particle’s position, imparts an unknown momentum to it via radiation pressure, which prevents one from predicting the outcome of a later position measurement, since the momentum and position do not commute. This is known as quantum back action. For a free mirror of mass M , the power spectral density of the minimum uncertainty in its position, given by the SQL, is $S_x^{SQL} = \frac{8\hbar}{M\Omega^2}$, where Ω is the angular frequency angular frequency at which the measurement is made. More generally, the SQL is the limit on the accuracy with which any position-sensing device can determine the position of a free mass.¹⁰

The SQL in interferometers with input power I_0 , which can also be stated as $S_x S_p \geq \hbar^2/4$, where $S_x \propto I_0$ is the power spectral density of position fluctuations due to the uncertainty in the number of photons (shot noise) and $S_p \propto 1/(I_0\Omega^2)$ is due to the backaction (radiation-pressure noise). We notice that the spectrum of the shot noise is flat, while that of radiation-pressure noise falls off as $1/\Omega^2$. This causes these two noise sources to dominate in different frequency bands. A further analogy between the position-momentum commutation and amplitude-phase commutation in quantum optics shows that the radiation-pressure noise and shot noise are associated with two orthogonal quadratures of the radiation field.

In initial LIGO interferometers, the input laser power is low enough that the sensitivity will be limited by shot noise, and radiation-pressure noise will be completely insignificant.

1.3. Quantum Non-demolition

A fundamental premise of the SQL is that is that the optical noise sources – radiation-pressure noise and photon shot noise – together enforce the SQL *only if they are uncorrelated*. The SQL can be overcome by creating correlations between the radiation-pressure and the shot noise. Quantum non-demolition (QND) devices, first proposed by Braginsky,¹¹ are generically measurement apparatuses that prevent their own quantum properties from ‘demolishing’ the state of the system they are performing a measurement on. QND interferometers are achieved by creating correlations between the radiation-pressure and shot-noise.

Here we discuss three ways in which QND interferometers can be realized:

- **Squeezed state injection**

Squeezed states of light reduce the noise in one quadrature at the expense of additional noise in the orthogonal quadrature. As mentioned above, vacuum fluctuations entering the unused port of the beam-splitter corrupt the measurement of the mirror position. Injecting squeezed vacuum with the appropriate squeeze quadrature into the unused port can reduce the dominant optical noise source, typically by a factor $S_h \propto e^{-2R}$, where e^{-2R} is the *power squeeze factor*. The *squeeze angle* governs the degree of squeezing in each quadrature.

- **Ponderomotive squeezing and the variational readout**

Ponderomotive squeezing arises from the naturally occurring correlation of light intensity fluctuations (radiation-pressure noise) to mirror position fluctuations (shot noise) upon reflection of light from a mirror. A heuristic description of this process is that when light (or vacuum) with fluctuations in the amplitude (radiation-pressure) quadrature, ΔI , and with fluctuations in phase quadrature, $\Delta\phi$, is incident on a mirror, the mirror position is influenced by ΔI due to the back-action force of the light on the mirror. If the position signal is measured in the phase quadrature, then the noise on that measurement is given by $\Delta\phi - \kappa(\Omega)\Delta I$, where $\kappa(\Omega)$ is measure of the back-action coupling and *depends on the frequency of oscillation of the mirror*, Ω . If a single quadrature is measured at the output of the interferometer, the noise on that measurement will depend on $\kappa(\Omega)$ at each frequency Ω . If, however, one could measure an admixture of quadratures with a *frequency-dependent* homodyne angle that is a function of κ , it is possible to completely eliminate ΔI from the measurement, at all frequencies.²⁶

- **Optical springs**

Another way to realize QND in an interferometer is by modification of the interferometer mirror dynamics by coupling to the light. The basis of this coupling is the fact that the radiation-pressure force not only imposes random fluctuations on the positions of the interferometer mirrors, but also exerts a restoring force with a deterministic frequency-dependent spring constant (sometimes called 'ponderomotive rigidity').¹⁸ The high-power optical field incident on the arm cavity mirrors of certain interferometer configurations gives rise to mirror dynamics that can be characterized by a pair of resonances: a low-frequency resonance due to the *mechanical* restoring force from the ponderomotive rigidity, and a higher-frequency *optical* resonance due to the light storage in the cavity.

2. INTERFEROMETER CONFIGURATIONS AND QND

The mechanisms by which the quantum noise couples to the GW signal at output port of the detector are strongly influenced by the interferometer configuration and the readout method used. Since the very earliest analyses of quantum noise in interferometers, the radiation-pressure noise and shot noise were assumed to be uncorrelated.^{6,12} This is largely true for a Michelson interferometer and certain variations, such as the power-recycled interferometer used in initial LIGO. However, with increased input and higher circulating power and the addition of a "signal recycling" optical cavity at the output port of the interferometer, it is possible to build up dynamical correlations between the shot noise and backaction noise.¹⁷

In order to fully explore the quantum noise in interferometers, detailed knowledge of the interferometer configuration is therefore necessary. In this section we outline a few configurations that are particularly useful to study, either because they are naturally QND interferometers or have the potential to be converted into QND interferometers.

In Fig. 1 we show schematics of some of the interferometer configurations we refer to in the sections that follow.

2.1. Power-recycled interferometers

In the initial LIGO detectors (as well as VIRGO and TAMA300), two km-scale Fabry-Perot cavities are inserted into the arms of the Michelson interferometer. Build-up of the optical field in the cavities enhances the GW-induced phase shift, thus increasing the sensitivity of the detector. The Michelson interferometer is operated on the dark fringe to minimize the shot noise associated with static laser power at the antisymmetric (dark) port. Since most of the light returns toward the laser, a partially transmitting power-recycling mirror (PRM) is placed between the laser source and the beam splitter to 'recycle' the light back into the interferometer¹⁴ (see Fig. 1(a)).

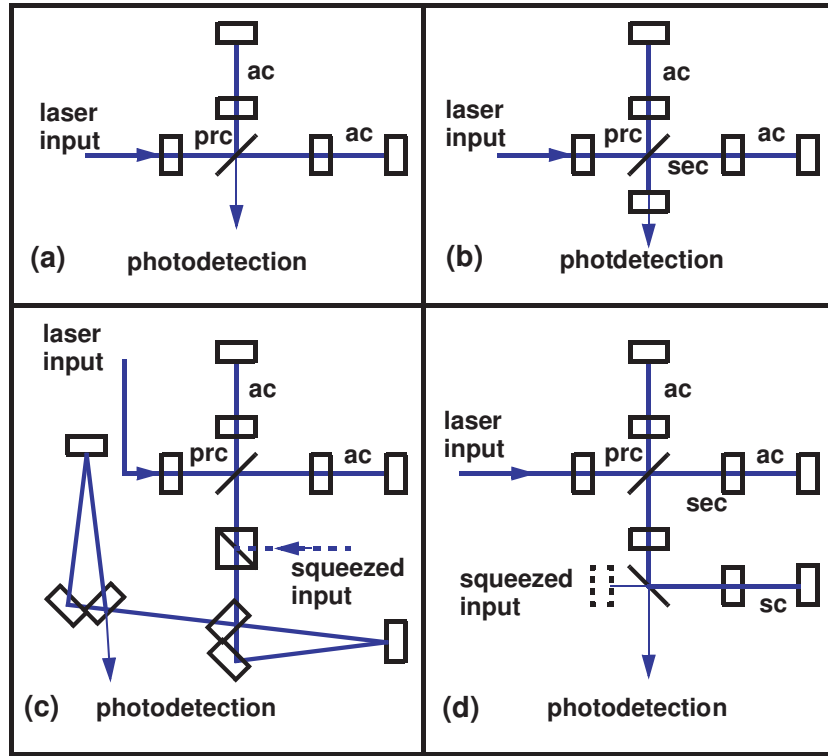


Figure 1. Schematic representations of some sample interferometer configurations. In all cases shown except (c) we have chosen extensions of a power-recycled Michelson interferometer with Fabry-Perot cavities in each arm as the basic interferometer; this configuration is shown in (a). (a) Power-recycled Michelson interferometer with Fabry-Perot arm cavities (PRFPMI); (b) Signal-tuned PRFPMI; (c) PRFPMI with variational readout and (optional) squeezed input; and (d) PRFPMI-based speed meter with (optional) squeezing. Acronyms used: ac = arm cavity, prc = power-recycling cavity, sec = signal extraction cavity, sc = sloshing cavity.

The GW signal at frequency Ω , due to the asymmetric motion of the end mirrors, appears as an phase modulation at the input coupler (ITM) of the arm cavities. Upon mixing with a local oscillator field at the beam splitter this phase modulation is converted to amplitude modulation that is detected by the photodetector. The GW signal appears *only* in a single quadrature.

The radiation-pressure noise and shot noise in this interferometer are uncorrelated, just as in a simple Michelson interferometer. Vacuum fluctuations entering the antisymmetric port of the beamsplitter pass into each arm and return to the antisymmetric port with an (uninteresting) overall phase shift. Even as the laser power in the interferometer is increased, the best performance that can be achieved is at the level of the SQL, unless squeezed light is injected into the unused port of the beamsplitter. Since there is an absence of QND at all powers under normal operating conditions, where signal in a single quadrature is measured, this configuration has been dubbed "conventional interferometer". Methods for converting this configuration into a QND interferometer via by cancellation of radiation-pressure and shot-noise are discussed in Section 3.2.

2.2. Signal-tuned interferometers

Signal-tuned interferometers are already used in the GEO600 detector, and are part of the baseline plan for the Advanced LIGO detectors.

The optical configuration currently planned to achieve quantum-limited performance in Advanced LIGO uses the Resonant Sideband Extraction (RSE) technique,¹⁵ in addition to power-recycling. In RSE, an additional partially transmitting mirror, the signal extraction mirror (SEM), is placed between the antisymmetric port

of the beam splitter and photodetector (see Fig 1(b)). The optical properties (reflectivity, loss) of this signal extraction mirror and its microscopic position (in fractions of the wavelength of the laser light, $1.064\text{ }\mu\text{m}$) can significantly influence the frequency response of the interferometer.¹⁶ The resonance condition of the signal extraction cavity – comprising the SEM and the input test-mass (ITM) mirrors of the arm cavities – and the reflectivity of the SEM control the frequency of peak response and the bandwidth of the detector, respectively.

The signal-recycling cavity is offset (detuned) from resonance to shift the frequency of the peak optical response of the detector to frequencies where other noise sources are not dominant. This detuning has the profound consequence, however, that the frequency response of the detuned configuration is no longer symmetric around the carrier frequency. As a consequence, only one of the two (upper or lower) GW-induced sidebands is exactly on resonance in the signal-recycling cavity. In general, the upper and lower GW sidebands contribute asymmetrically to the total output field, *which makes the GW signal appear simultaneously in both quadratures of the output field*.¹⁷

To achieve quantum-limited performance, the optical configuration for Advanced LIGO includes not only the SEM at the antisymmetric output of the interferometer but also much higher circulating powers. The higher circulating power immediately enhances the role of radiation pressure noise in the overall noise performance of the interferometer. Furthermore, use of the detuned RSE to optimize the detector response has exposed some surprising features that are due to the dynamical correlations of the shot noise and radiation pressure noise.¹⁷ These shot noise–radiation pressure noise correlations – which are manifestations of quantum non-demolition (QND) in that the correlations lead to below-SQL noise limits – lead to an opto-mechanical coupling that significantly modifies the dynamics of the interferometer mirrors, introducing an additional resonance at which the sensitivity also peaks (see, e.g., the dark solid (blue) curve in Fig. 3).^{17,18}

2.3. Third-generation interferometers

Several novel interferometer configurations have been proposed for GW detectors beyond Advanced LIGO. These include all-reflective interferometers, which circumvent the problems associated with thermal distortions due to the heat deposited in the absorptive substrates of mirrors when laser beams pass through them; white light interferometers which are capable of extremely broadband operation; and a class of back-action evading interferometers, known as *speed meters*. We will limit our discussion to speed meters since they are inherently QND devices. Furthermore, we defer that discussion till Sec. 3.2.

3. PROSPECTS FOR SQUEEZING

Since the earliest experiments to generate squeezed states of light were carried out in the 1980's,^{19,20} there has been steady progress in both the degree of squeezing achieved²¹ as well as the stability and long-term operation of squeezing experiments.²² The use of squeezed light in various applications has nudged squeezed state generation from delicate laboratory set-ups with millisecond durations to the realm of stable sources of strongly squeezed light that operate robustly for several hours at a time. The present state of the art for CW squeezed light is about 6 dB of squeezing at several 100 kHz.

3.1. Squeezed state generation

For squeezed light to be useful in GW interferometers there are a few major directions in which the state-of-the-art must progress:

- **Increased level of squeezing**

A benchmark for squeezing to become a viable technology for GW detectors is squeeze factors of greater than 10 dB. This requirement is a great challenge but one that has seen steady but slow progress. One of the most promising techniques for squeeze source generation continues to be the $\chi^{(2)}$ non-linearity in crystals. One example of known limitations with $\chi^{(2)}$ non-linear materials is green-induced infrared absorption – or GRIIRA – in LiNbO_3 , which is often cited as a limitation to the degree of squeezing as well as deviations from theoretical optimizations in OPAs. Absorption measurements of MgO-doped LiNbO_3 have shown a strong dependence of GRIIRA on both the stoichiometry and on the MgO concentrations.²⁴ In fact, the

results indicate that carefully control of these two effects can all but eliminate GRIIRA (and photorefraction, as an added side-effect). This is an area of development where new materials and improvements in the growth parameters of next-generation crystals will contribute to the elusive 10 dB goal.

- **Squeezing at low frequencies**

Broadband cw squeezing is presently available at frequencies above about 300 kHz.²⁵ This is, of course, not useful for GW interferometers that need quantum-limited operation at around 100 Hz. There are two primary factors which give rise to the present frequency limit: (i) Classical noise on the seed beam, i.e. the seed beam is not shot-noise-limited at frequencies below about 1 MHz; and (ii) Noise introduced inside the non-linear devices used for squeezing, e.g. in the optical parametric amplifiers (OPAs).

The first limitation is not particularly relevant for squeezed *vacuum*, which is all that is required for injection into the unused ports of gravitational-wave interferometers. Recently, there has also been some progress on the second limitation, regarding noise generated in OPAs. Classical laser noise is still a problem in that it couples to the squeezed output beam via experimental imperfections such as crystal non-uniformities and mode-mismatch. One approach is to facilitate noise cancellations by passing both the pump beam and the seed beam through a pair of OPAs.²⁵ Careful control of the relative phases of the beams allows for cancellation of the classical noise on the laser. This technique has led to realizing squeezing in the 200 kHz band, but continues to be limited by technical noise due to the imbalance between the two OPAs and uncorrelated acoustic noise in the OPAs. A technique for eliminating this latter is effect is proposed by use of a ring OPA to classically correlate the noise on each of the squeezed outputs that are counter-propagating in the ring OPA.²⁵

- **Lowering losses**

Another area of development for increasing the squeezing efficiency is the minimization of other losses in the system. These include photodetection efficiency and optical losses that destroy the hard-earned quantum correlations on the squeezed light. In Section 3.2, we highlight the effects of a variety of losses in a GW detector with squeezing.

3.2. Applications of squeezing to gravitational-wave interferometers

In this section we describe some of the effects of using squeezed light in GW interferometers. We assume availability of 10 dB of vacuum squeezing available from DC to 10 kHz. 10 dB corresponds to the squeeze factor $e^{-R} = 0.3$. Here we do not include losses, but the effect of losses are described in Sec. 4. We consider the use of squeezed light in:

3.2.1. Power-recycled interferometers

Several variations have been proposed to turn these "conventional" interferometers into QND devices. The sensitivity curves for these are shown in Fig. 2.

- In the *squeezed-input interferometer* squeezed vacuum is injected into the antisymmetric port of the interferometer. Squeezing has the effect of increasing the fluctuations in one quadrature, while decreasing fluctuations in the other. The *squeeze angle* describes the linear combination of input quadratures in which the fluctuations are reduced. Since radiation-pressure noise and shot noise dominate in different frequency regions and depend on different input quadratures, the squeeze angle that achieves optimal performance is frequency dependent. A possible configuration is choosing a frequency independent squeeze angle that decreases shot noise and increases radiation pressure noise. This configuration is equivalent to an unsqueezed interferometer with an increase to the laser power by the squeeze factor.⁷ To obtain a broadband performance increase, two km-scale(required for low losses) Fabry-Perot filter cavities can produce the required frequency dependent squeeze angle from a fixed squeeze angle source. In this configuration, the noise(power) is reduced by the squeeze factor at all frequencies.
- In the *squeezed-variational interferometer* two km-scale Fabry-Perot filter cavities to perform a frequency dependent homodyne detection of the signal. This detection method eliminates radiation-pressure noise from the signal by creating correlations between the shot noise and radiation-pressure noise. As a result,

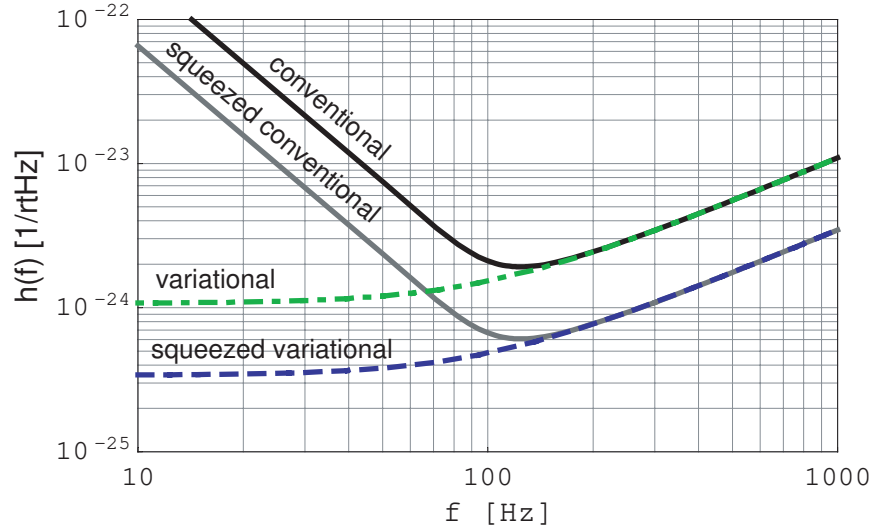


Figure 2. Noise curves for a power-recycled interferometer (with initial LIGO parameters) with squeezing and with a variational readout.²⁶ The solid dark (black) curve uses the standard, or baseline, initial LIGO parameters but power at the beamsplitter that gives SQL-limited performance at 100 Hz, i.e. ($I_0 = I_{SQL} \simeq 10$ kW; the solid light (gray) curve is the sensitivity for the same interferometer but with squeezing injected at a *frequency-dependent* optimal squeeze angle; the dash-dot (green) curve is for the same interferometer but using a *frequency-dependent* homodyne readout that measures the optimal quadrature at each frequency; the lighter dashed curve (blue) uses a variational readout as well as 10 dB of squeezing injected. No losses are included in the noise curves plotted here, but the treatment including losses can be found in Ref. [26].

squeezing must only reduce the shot noise, and the radiation-pressure noise may be disregarded, which results in a frequency independent squeeze angle and the noise (power) is reduced by the squeeze factor at all frequencies.

3.2.2. Signal tuned interferometers

The results shown in this section are a preview of work that appears in a manuscript we are preparing for submission.²⁷ We limit our discussion to the detuned RSE interferometers planned for Advanced LIGO and show that there are reasonable gains to be made even with frequency-independent squeezing.

The introduction of signal recycling has the effect of mixing the quadratures in the input/output relations of the interferometer. This allows the shot noise and radiation pressure noise to become correlated, producing the two well known resonances typical of signal recycled interferometers.¹⁷

To improve the performance of this configuration, we inject squeezed vacuum into the dark port. The mixing of the quadratures results in the optimal squeeze angle being modified from the power-recycled case. It has been shown that this frequency-dependent squeeze angle can be produced by kilometer scale filter cavities.^{26,35} Due to the inherent difficulty of using long filter cavities, we will consider the case of a fixed squeeze angle in the Advanced LIGO configuration.

For the standard detuning of the signal recycling cavity in Advanced LIGO, the resonances are placed near 100 Hz to achieve the best performance in the frequency range with the best sensitivity. This results in the optimal squeeze angle being strongly frequency dependent and in making broadband improvements impossible. By choosing the optimal squeeze angle for a particular frequency band, narrowband improvements can be achieved, at the cost of worse performance at other frequencies. To increase the broadband performance, we must modify the detuning of the signal recycling cavity so as to reduce the variance of the optimal squeeze angle. We choose a detuned signal extraction cavity, such that carrier light with angular frequency ω_l obtains a net phase shift of $\frac{\pi}{2}$ in one pass through the cavity. In this configuration, the optimal squeeze angle varies much less than

in the standard configuration. We choose a squeeze angle to optimize the noise performance at 200 Hz. This choice allows us to improve the performance over the bulk of our frequency range. The performance of the squeezed configuration is comparable to the unsqueezed configuration in the frequency range 10 Hz to 300 Hz, and dramatically better at 300 Hz to 10 kHz.

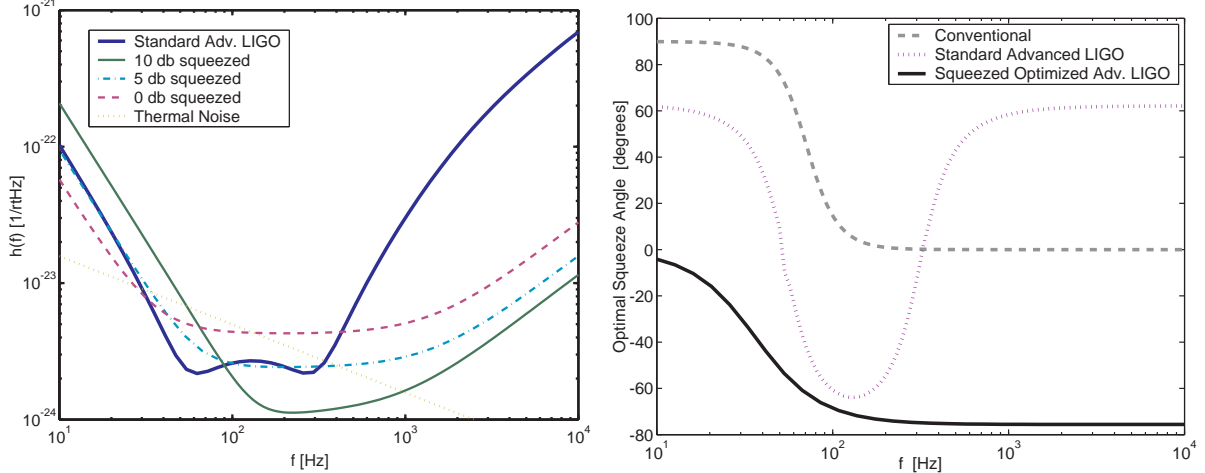


Figure 3. Right panel: Noise curves for Advanced LIGO with different levels of squeezing included.²⁷ The dark solid curve is the standard, or baseline, Advanced LIGO sensitivity when limited by quantum noise; the dashed (purple) curve corresponds to a broadband configuration that is better suited for squeezing (but no squeezing is injected); the dash-dot (cyan) curve is for the broadband configuration with 5 dB of squeezing; the lighter solid curve (green) has 10 dB of squeezing injected. The dotted (yellow) curve is an estimate of the thermal noise, assuming 40 kg silica test masses limited by internal thermal noise.³ Left panel: The optimal squeeze angle for three interferometer considered. The dashed curve (gray) is for a conventional power-recycled interferometer; the dotted curve (purple) is for the standard (baseline) Advanced LIGO configuration; the solid (black) curve is for the optimized broadband advanced LIGO configuration.

3.2.3. Speed meters

The principle of a "speed" meter is most easily understood in terms of the HUP applied to position and momentum. In Section 1.2, we highlighted how a position measurement at time t_0 disturbs a consequent measurement at a later time $t_1 > t_0$ due to the momentum "kick" from the first measurement. This back-action obviously does not make position a very good QND observable. While a measurement of momentum certainly perturbs the position of a test particle as required by the HUP, that position "kick" does not influence the time evolution of the momentum, and hence there is no back-action. Momentum measurements are thus inherently back-action evading *, provided no position information is collected. Interferometric measurements that measure the *speed* – similar in behavior to the *momentum* – of the mirrors were first proposed by Braginsky et al.³⁶ and refined into more practical designs by Purdue and Chen.^{4,5}

Many Michelson-based variants of interferometric speed meters rely on the addition of a "sloshing" cavity at the output port of an otherwise position sensitive interferometer. The role of the "sloshing" cavity is to completely cancel the momentum "kick" due to the position measurement at t_0 by an equal and opposite "kick" at $t_0 + \tau_s$, where τ_s is the storage time of the sloshing cavity. Optically, this occurs due to a π phase shift in the coupling constant that connects the sloshing cavity field to the interferometer field. This behavior is quite analogous to that of two weakly coupled oscillators: when something other than a normal mode of the system is excited, energy "sloshes" between the two oscillators, with a π phase shift after each "slosh" cycle.³³ A schematic representation of a sample speed meter interferometer is shown in Fig. 1(d). The unused port of the readout mirror that connects the sloshing cavity (sc) to the signal extraction cavity (sec) can with be plugged (with the

*Momentum, or velocity, is a constant of the motion for a free particle; it commutes with itself at different times and is, therefore, a good QND variable.

dashed mirror), or it can be used for squeezed vacuum injection. We do not include noise curves corresponding to various speed meter configurations here, but these appear aplenty in Ref. [4].

4. THE ROLE OF LOSSES

Optical losses play an important role in the performance of a squeezed interferometer. There are two mechanisms that must be considered in simultaneously when evaluating the effects of losses: (i) The dissipation leads to smaller signals, which is purely classical effect; and (ii) A lossy port allows ordinary (unsqueezed) vacuum to enter and superpose on the squeezed field in the interferometer, thus destroying the effects of the squeezing.

In general, the significance of the different losses in an interferometer or associated injection/readout scheme depends on the interferometer configuration. Squeezed light injection losses are obviously problematic, since they correspond to pure degradation of the level of squeezing. The sensitivity to optical losses in an interferometer depends on the build-up of signal and noise fields in the various part of the interferometer. In the variation and/or squeezed-variational interferometer of Fig. 1(c), for example, the losses in the arm cavities dominate the overall performance of the detector.²⁶

In this section we consider the effect of losses in the signal-tuned interferometer described in Sec. 3.2, as an example.²⁷ The effects of the losses is strongly dependent on the buildup of the noise fields in the signal extraction cavity and in the arm cavities. There are four types of losses we consider:

- *Injection losses* are losses associated with the injection of squeezed light into the dark port. This effectively limits the squeezing magnitude, and we assume that these are included in the squeezing magnitudes used and are subsequently ignored.
- *Detection losses* are due to quantum inefficiencies in the detection of the signal light. These losses allow a small amount of vacuum fluctuations to leak into the measurement, decreasing its precision. The vacuum fluctuations are small relative to the radiation pressure noise at low frequencies and thus has little effect where radiation pressure noise dominates. The vacuum fluctuations are significant relative to shot noise, however, and hurt performance at high frequencies where shot noise dominates.
- *Signal recycling losses* are produced by the beamsplitter, signal recycling mirror, and the anti-reflective coatings on the initial test masses. These losses are either amplified or suppressed depending on the buildup of the noise fields in the signal extraction cavity. The frequency-dependent phase shift experienced by the noise fields in interacting with the arm cavities results in the signal recycling cavity being resonant at high frequencies, and anti-resonant at low frequencies, and thus the effects of the losses is amplified at high frequencies and suppressed at low frequencies.
- *Arm cavity losses* are incurred in the arm cavities due to diffraction and absorption. Due to the suppression of the noise fields at low frequencies in the signal recycling cavity, and to the suppression of the noise fields at high frequencies in the arm cavities, the noise fields do not resonate strongly in the arm cavities. This effect reduces the importance of arm cavity losses.

While not apparent from Fig. 4, we have determined that the dominant losses in this configuration arise from the *signal recycling cavity*, and that the effects of the losses are the worst at frequencies above 300 Hz and limit the amount of squeezing that is beneficial at these frequencies. The losses are largely unimportant at frequencies below 300 Hz. As mentioned above, these effect of these losses is amplified or suppressed, depending on the resonance condition in the signal extraction cavity.

5. THE CHOICE OF READOUT SCHEME

Since GW interferometers operate on a dark fringe, the intensity of the light exiting the antisymmetric port is quadratic in the GW amplitude, and therefore insensitive to it, to first order. The standard way to circumvent this is to interfere the signal field with a relatively strong local oscillator (LO) field, such that the intensity of the total optical field, detected at the beat frequency, varies linearly with the GW amplitude. The various methods of measuring the GW-induced signal at the antisymmetric port are referred to as *readout schemes*.

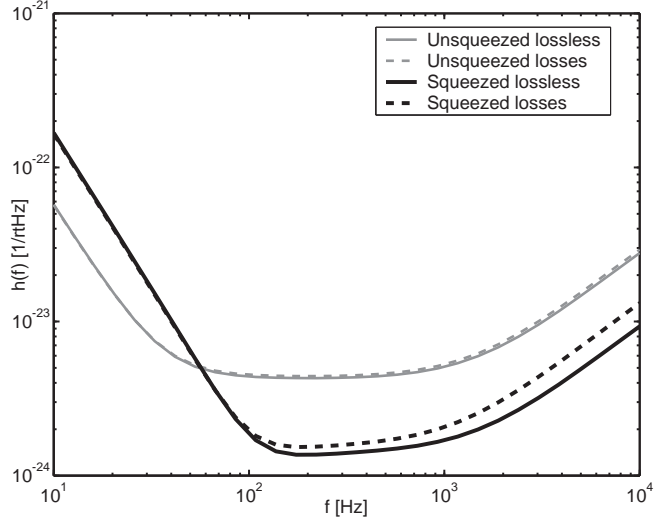


Figure 4. Noise curves for a squeezed input signal-tuned interferometer (with broadband Advanced LIGO parameters) including losses.²⁷ The solid gray curve is for the broadband Advanced LIGO configuration shown as the dashed (purple) curve in Fig. 3; the dashed gray curve is the sensitivity for the same interferometer but with additional losses (see below) ; the solid black curve is for the lossless interferometer squeezing injected (same as the lighter solid (green) curve of Fig. 3; the dashed curve black curve includes losses. The losses assumed in these curves are 50 ppm per high-reflection surface, 200 ppm per anti-reflection surface and photodetection efficiency of 98%.

Our discussion thus far has been limited to homodyne detection, where the beat between the optical signal field at frequencies ($\omega_l \pm \Omega$) and the carrier field at frequency ω_l is detected (i.e. the LO field oscillates at exactly the same frequency as the incident laser). Here $\omega_l \sim 2 \times 10^{15}$ refers to the laser frequency, while $\Omega \sim 10 - 10000$ Hz is the frequency of the GW. It is worth commenting on the viability of heterodyne readout schemes, in which the LO has different frequencies from the carrier. The heterodyne readout is usually implemented, as in initial LIGO, by using phase modulated light: the light incident on the interferometer consists of a carrier at ω_l and radio frequency (RF) phase modulation (PM) sidebands at frequencies $\omega_l \pm \omega_{RF}$. The PM sidebands are transmitted with maximum efficiency to the antisymmetric port via Schnupp asymmetry,³⁰ while the carrier still returns to the symmetric port. The transmitted sidebands then act as a LO against which the GW signal can beat, generating signals at $\pm(\omega_{RF} \pm \Omega)$. Demodulation at ω_{RF} converts the signal back down into the baseband.

The heterodyne readout scheme has some advantages: (i) laser technical noise can be circumvented by upconverting the signal detection to frequencies where the laser light is shot-noise-limited (a few MHz); and (ii) more than one quadrature of the interferometer output can be measured [†]. The latter attribute is of great importance in detuned RSE interferometers, where the GW signal appears in *both* quadratures, and *the optimal detection quadrature is frequency-dependent*.

Unfortunately, there is also a fundamental disadvantage: an *additional* contribution to the quantum noise due to vacuum fluctuations in frequency bands that are twice the modulation frequency away from the carrier, as compared with the homodyne readout scheme. This effect was studied extensively for detection of a single (phase) quadrature,^{12, 13, 30-32} which is adequate for interferometers with low circulating power, and hence negligible back action noise.

Recently, the heterodyne readout scheme was generalized to detection of generic quadratures with LO light that is an arbitrary mixture of phase and amplitude modulation, more applicable to advanced GW detectors.³⁴ This analysis led to some startling general results. The additional heterodyne noise is a direct consequence of the HUP: as long as more than one quadrature is available for simultaneous measurement, the additional heterodyne

[†]We refer to this as "variable-quadrature heterodyne detection" after Ref. [34]

noise will appear. Moreover, the HUP imposes a quantum limit to the additional heterodyne noise, which is independent of frequency (unless frequency-dependent squeezing is implemented). This frequency-independent quantum limit puts hard constraints on the ability of the variable-quadrature optimization afforded by heterodyne schemes to achieve QND performance over a broad range of frequencies.

6. CONCLUSION

We have attempted to give a very broad survey of recent developments in our understanding of quantum noise in gravitational-wave interferometers. With regard to laser interferometer gravitational-wave detectors, the stage was set in the late 1970s and early 1980s by the work of Caves, Thorne, Braginsky et al., and many, many others, which introduced the conceptual and mathematical formulation of the problem of quantum noise limits in macroscopic measurements and the possibility of circumventing them by quantum non-demolition techniques, using squeezed light, for example. These ideas were deemed not to be realizable in GW detectors at the time [‡]. In the following decade, there were significant enough advances in the generation of non-classical states of light^{19, 20, 22, 23} and their use to make modest gains in interferometric measurements below the quantum limit,^{28, 29} that once again renewed interest in the topic at the turn of the millennium. The work of Buonanno and Chen,^{17, 18} building on that of Kimble et al.,²⁶ led to better understanding of the important role that naturally occurring quantum correlations can play in advanced GW detectors with higher power, hence non-negligible back action noise. At the present time, we have entered an era of vigorous activity and interest in possibility of sub-SQL measurement techniques that aim to take advantage of (i) squeezed-state generation and injection; (ii) the naturally occurring ponderomotive squeezing in interferometers; (iii) other back action evading measurement techniques based on speed meters^{4, 5}; and a variety of other techniques that we have not described here [§].

ACKNOWLEDGMENTS

We thank Stan Whitcomb and Yanbei Chen for their invaluable comments/corrections to this manuscript, and our colleagues at the LIGO Laboratory for many valuable discussions. The LIGO Observatories were constructed by the California Institute of Technology and Massachusetts Institute of Technology with funding from the National Science Foundation under cooperative agreement PHY-9210038. The LIGO Laboratory operates under cooperative agreement PHY-0107417.

REFERENCES

1. A. Abramovici et al., “LIGO – the laser interferometer gravitational-wave observatory,” *Science* **256**, pp. 325–333, 1992 (<http://www.ligo.caltech.edu>);
B. Caron et al., *Class. Quantum Grav.* **14**, p. 1461, 1997 (<http://www.virgo.infn.it>);
H. Lück et al., *Class. Quantum Grav.* **14**, p. 1471, 1997 (<http://www.geo600.uni-hannover.de>);
M. Ando et al., *Phys. Rev. Lett.* **86**, p. 3950, 2001 (<http://tamago.mtk.nao.ac.jp>).
2. G. Sanders, “Status of LIGO,” in *Gravitational Wave Detection, Proc. SPIE* **4856-35**, p. 247, 2002.
3. P. Fritschel, “Second generation instruments for the Laser Interferometer Gravitational-wave Observatory (LIGO),” in *Gravitational Wave Detection, Proc. SPIE* **4856-39**, p. 282, 2002.
4. P. Purdue and Y. Chen, “Practical speed meter designs for QND gravitational-wave interferometers,” *Phys. Rev. D* **66** pp. 022001, 2002 ([gr-qc/0208049](http://arxiv.org/abs/gr-qc/0208049)).
5. G. DeVine, M. Gray, D. McClelland, Y. Chen, and S. Whitcomb, private communication (<http://www.ligo.caltech.edu/docs/G/G030087-00/G030087-00.pdf>).
6. C. M. Caves, “Quantum-mechanical radiation-pressure fluctuations in an interferometers,” *Phys. Rev. Lett.* **45**, pp. 75–78, 1980.

[‡]In the Conclusions section of his 1981 paper,⁷ Caves wrote: “The squeeze-state technique outlined in this paper will not be easy to implement... Difficult or not [it] might turn out at some stage to be the only way to improve sensitivity of detectors designed to detect gravitational waves...”

[§]The authors apologize in advance to groups and individuals who made pivotal contributions to the developments mentioned here that we did not have time/scope to mention.

7. C. M. Caves, "Quantum-mechanical Noise in interferometers," *Phys. Rev. D* **23**, pp. 1693–1708, 1981.
8. V. Braginsky, M. Gorodetsky, F. Khalili, A. Matsko, K. Thorne, and S. Vyatchanin, "The noise in gravitational-wave detectors and other classical-force measurements is not influenced by test-mass quantization," gr-qc/0109003 (2001).
9. V. B. Braginsky and F. Ya. Khalili, *Rev. Mod. Phys.* **68**, p. 1, 1996.
10. V. B. Braginsky and F. Y. Khalili, "Quantum Measurement," K. S. Thorne, ed., Cambridge University Press, Cambridge, 1992.
11. V. B. Braginsky and Yu. I. Vorontsov, *Sov. Phys. - Uspekhi* **17**, p.644, 1975.
12. B. Meers and K. A. Strain, "Modulation, signals and and quantum noise in interferometers," *Phys. Lett. A* **44**, pp. 4693–4703, 1991;
13. T. M. Niebauer, R. Schilling, K. Danzmann, A. Rdinger, and W. Winkler, "Non-stationary noise and its effect on the sensitivity of interferometers," *Phys. Rev. A* **43**, p. 5002, 1991.
14. R. W. P. Drever, in *The detection of gravitational waves*, D. G. Blair, ed., Cambridge University Press, Cambridge, England, 1991.
15. J. Mizuno, "Comparison of optical configurations for laser-interferometer gravitational-wave detectors," Ph.D. thesis, Max-Planck-Institut für Quantenoptik, Garching, Germany, 1995.
16. J. Mason and P. Willems, "Signal extraction and optical design for an advanced gravitational-wave interferometer," *Appl. Opt.* **42**, 1269 (2003); see also K. A. Strain, G. Muller, T. Delker, D. H. Reitze, D. B. Tanner, J. E. Mason, P. Willems, D. Shaddock, M. B. Gray, C. Low-Mowry, and D. E. McClelland , "Signal and control in dual-recycling laser interferometer gravitational-wave detectors," *Appl. Opt.* **42**, 1244 (2003).
17. A. Buonanno and Y. Chen, "Quantum noise in second-generation signal-recycled laser interferometric gravitational wave detectors," *Phys. Rev. D* **64**, p. 042006 (2001).
18. A. Buonanno and Y. Chen, "Signal recycled alser-interferometer gravitational-wave interferometers as optical springs," *Phys. Rev. D* **65**, p. 042001, 2002;
19. R. E. Slusher, L. W. Holberg, B. Yurke, J. C. Mertz, and J. F. Valley, "Observation of squeezed states generated by four-wave mixing in an optical cavity," *Phys. Rev. Lett.* **55**, pp. 2409 (1985).
20. L.-A. Wu, H. J. Kimble, J. L. Hall, and H. Wu, "Generation of squeezed states by parametric down-conversion," *Phys. Rev. Lett.* **57**, pp. 2520–2523 (1986).
21. S. Schiller, G. Breitenbach, S. F. Periera, T. Müller and J. Mlynek, Quantum statistics of the squeezed vacuum by measurement of the density matrix in the number state representation," *Phys. Rev. Lett.* **77**, p. 2933, 1996.
22. K. Schneider, M. Lang, J. Mlynek, S. Schiller, "Generation of strongly squeezed continuous-wave light at 1064 nm," *Opt. Exp.* **2**, pp. 59–64 (1998).
23. P. K. Lam, T. C. Ralph, B. C. Buchler, D. E. McClelland, H.-A. Bachor, and J. Gao, "Optimization and transfer of vacuum squeezing from an optical parametric oscillator," *J. Opt. B - Quant. Semiclass. Opt.* **1**, p. 469, 1999.
24. Y. Furakawa, K. Kitamura, A. Alexandrovski, R. K. Route, and M. M. Fejer, "Green-induced infrared absorption in MgO doped LiNbO₃," *Appl. Phys. Lett.* **78**, pp. 1970–1972, 2001.
25. W. P. Bowen, R. Schnabel, N. Treps, H.-A. Bachor, and P. K. Lam, "Recovery of continuous wave squeezing at low frequencies," quant-ph/0205097 (2002).
26. H. J. Kimble, Yu. Levin, A. B. Matsko, K. S. Thorne, and S. P. Vyatchanin, "Conversion of conventional gravitational-wave interferometers into QND interferometers by modifying their input and/or output optics," *Phys. Rev. D* **65**, p. 022002, 2002.
27. T. Corbitt and N. Mavalvala, "Optimization of the Advanced LIGO detector to include squeezing," in preparation, 2003.
28. M. Xiao, L.-A. Wu, and H. J. Kimble, "Precision measurement beyond the shot noise limit," *Phys. Rev. Lett.* **59**, pp. 278–281, 1987.
29. K. McKenzie, D. A. Shaddock, D. E. McClelland, B. C. Buchler, and P. K. Lam, "Experimental demonstration of a squeezing-enhanced power-recycled Michelson interferometer for gravitational-wave detection," *Phys. Rev. Lett.* **88**, p. 231102, 2002.

30. L. Schnupp, unpublished talk presented at the “European Collaboration Meeting on Interferometric Detection of Gravitational Waves,” 1988, Sorrento, Italy.
31. J. Gea-Banacloche and G. Leuchs, “Squeezed states for interferometric gravitational-wave detectors,” *J. Mod. Opt.* **34**, p. 793–811, 1987.
32. V. Chickarmane, S. V. Dhurandhar, T. C. Ralph, M. Gray, H.-A. Bachor, and D. E. McClelland, “Squeezed light in a frontal-phase-modulated signal-recycled interferometer,” *Phys. Rev. A* **57**, pp. 3898–3912, 1998.
33. P. Purdue and Y. Chen, private communication, 2003.
34. A. Buonanno, Y. Chen, and N. Mavalvala, “Quantum noise in laser-interferometer gravitational-wave detectors with a heterodyne readout scheme,” accepted to *Phys. Rev. D*, 2003 (gr-qc/0302041).
35. J. Harms, Y. Chen, S. Chelkowski, A. Franzen, H. Vahlbruch, K. Danzmann, R. Schnabel, “Squeezed-input, optical-spring, signal-recycled gravitational-wave detectors,” gr-qc/0303066.
36. V. B. Braginsky and F. Ya. Khalili, “Speed...,” *Phys. Lett. A* **147**, p. 251, 1990; V. B. Braginsky, M. L. Gorodetsky, F. Ya. Khalili, K. S. Thorne, “Dual resonator speed meter for a free test mass,” *Phys. Rev. D* **61**, p. 044002, 2000.